

Effect of Extruder Type on the Properties and Morphology of Reactive Blends Based on Polyamides

B. MAJUMDAR,* H. KESKKULA, and D. R. PAUL†

Department of Chemical Engineering and Center for Polymer Research, University of Texas at Austin, Austin, Texas 78712

SYNOPSIS

The morphology and mechanical properties of polyamide-based blends prepared in single and corotating twin-screw extruders were compared using transmission electron microscopy (TEM) techniques. Reactive polyamide blends with SEBS-*g*-MA (a maleated styrenic triblock copolymer with ethylene-butylene midblocks), EPR-*g*-MA (a maleated ethylene/propylene rubber), and ABS were selected for the purpose of this investigation. For blends of SEBS-*g*-MA with *difunctional* (nylon *x,y*) polyamides (e.g., nylon 6,6; nylon 12,12), the twin-screw extruder was more effective in producing a finer dispersion of the rubber phase, which resulted in a significant lowering of the ductile-brittle transition temperature in case of the nylon 6,6 blend. On the other hand, blends of SEBS-*g*-MA with the *monofunctional* nylon 6 material led to rubber particles that were too small for toughening for both extruder types employed in this work. For nylon 6/EPR-*g*-MA blends, the single-screw extruder led to blends with excellent low-temperature impact properties for both single-step and masterbatch mixing techniques, whereas nylon 6/EPR-*g*-MA blends prepared in a single-step operation in the twin-screw extruder were brittle under ambient conditions. For difunctional polyamide blends with ABS (compatibilized with an imidized acrylic polymer), the morphology and mechanical properties were found to be independent of the extruder type employed for processing. © 1994 John Wiley & Sons, Inc.

INTRODUCTION

Recent studies on polyamide blends with functionalized styrenic block copolymers, prepared in a laboratory single-screw extruder, have revealed important differences in phase morphology and mechanical properties depending on the chemical characteristics of the polyamide phase.¹⁻⁷ The size and shape of the dispersed domains of a maleated triblock copolymer of styrene/ethylene-butylene/styrene (SEBS-*g*-MA) were found to be strongly influenced by whether the polyamide had just one amine end group per chain (monofunctional, e.g., nylon *x*) or a fraction of the chains had two amine end groups (difunctional, e.g., nylon *x,y*). When the

polyamide matrix is monofunctional, regular spherical particles of SEBS-*g*-MA with diameters of the order of 0.05–0.15 μm are formed,¹⁻⁷ whereas difunctional polyamide matrices generate much larger, complex shapes with significant occlusions of the nylon material inside them.⁵⁻⁷

Here we explore the effects of more intensive compounding conditions on the morphology and mechanical properties of various blends based on monofunctional vs. difunctional polyamides. Specifically, reactive blends of SEBS-*g*-MA/SEBS,¹⁻⁷ ABS,⁹⁻¹¹ and a maleated ethylene propylene rubber (EPR-*g*-MA)¹² with various polyamides prepared in corotating twin-screw extruders are compared to the same compositions made in a single-screw extruder.

BACKGROUND

There have been numerous attempts to understand the complex shear and elongational flow fields along

* Present address: Department of Chemical Engineering and Material Science, University of Minnesota, 151 Amundson Hall, 421 Washington Avenue S.E., Minneapolis, MN 55455-0132.

† To whom correspondence should be addressed.

the various sections of both single- and twin-screw extruders.¹³⁻²⁵ Both theoretical and experimental approaches have shown that viscosity, elasticity, interfacial tension, intensity of mixing, and thermal history play an important role in controlling blend morphology.²⁶⁻⁵⁶ Relatively simple models based on the Taylor theory of drop breakup, originally devised for Newtonian fluids, have often been utilized as a framework for explaining dispersion phenomenon for polymer blends in complex viscoelastic flow fields in polymer blends. Correlations of the following form have been constructed for simple shear flow^{34,35}:

$$\eta_m G d / \gamma = F(\eta_d / \eta_m) \quad (1)$$

where γ is the interfacial tension; G , the shear rate; η_m , the viscosity of the matrix phase; and η_d , the viscosity of the dispersed phase. Thus, if all other factors are the same, the particle diameter, d , should be inversely proportional to the shear rate:

$$d \sim 1/G \quad (2)$$

In reality, elongational flow fields, in addition to shear flow, exist within intensive mixing devices like extruders, which, according to several investigators, may be more effective in controlling particle size under some conditions.³⁹⁻⁴⁵ Melt elasticity is frequently neglected in such analyses but can be an important factor in the final morphology of multiphase polymer blends.^{37,38} Some attempts have also been made to quantify the coalescence phenomenon that occurs during processing using models based on Smoluchowski's theory for aqueous colloid suspensions.^{46,47} These models predict an increase in phase size with dispersed phase concentration,⁴⁸⁻⁵⁰ which has been repeatedly observed experimentally.^{30-33,49} Simple models based on shear flow fields inside twin-screw extruders have been proposed for the semiquantitative prediction of blend morphology.²⁶⁻²⁹

The effect of the mixing process on morphology development in polymer blends has been described by several authors^{20,21,51-56}; however, most of these studies have employed nonreactive systems. In general, corotating twin-screw extruders lead to more effective control of blend morphology compared to that achieved in single-screw extruders because of their more intensive mixing, better control over the residence time, self-wiping of the screws, and better heat-transfer characteristics. In addition, twin-screw extruders are generally starve-fed in contrast to the flood feeding in conventional single-screw extruders, which allows an extra degree of control in the mixing independent of the screw speed. As evident from eq.

(2), more intense mixing or a higher shear rate should lead to a reduction in the dispersed phase particle size. For reactive systems, generation of a greater amount of an interfacial area should increase the probability of reaction and, thus, result in even greater changes in morphology.⁵⁷⁻⁶⁹

It has been demonstrated in our recent work that the particle size could be varied by over two orders of magnitude by only changing the extent of the graft copolymer formed at the polymer-polymer interface while maintaining the same processing conditions.⁵⁻⁷ It was also proposed that the topology of grafting plays an important role in determining the final morphology of the blend.¹⁻⁷ These differences stem from the differences in the grafting reactions that occur depending on whether the polyamide has one or two amine groups per chain to react with the anhydride units of the maleated rubber. The single-end grafting of polyamide chains to the reactive rubber that occurs with monofunctional polyamides is most effective for breaking up the rubber particles and preventing their coalescence, whereas the two-end grafting that is possible for difunctional polyamides leads to cross-linking-type effects and results in particles that are harder to break up and disperse in the matrix.⁷

In the nylon x series, the extremely small rubber particles generated by blending with SEBS-*g*-MA are below a critical size limit for toughening in the case of nylon 6 but in an optimum range for toughening for polyamides with higher CH₂/NHCO ratios in their repeat units, which leads to higher inherent matrix ductility. For nylon 6, it was necessary to dilute the SEBS-*g*-MA rubber with its unmaleated precursor, SEBS, for generating tough blends.¹⁻⁷ In the nylon x,y series, increasing the polyamide CH₂/NHCO led to smaller particles and lower ductile-brittle transition temperatures.⁷

Other recent work⁹⁻¹¹ on nylon/ABS blends prepared in a single-screw extruder and compatibilized with an imidized acrylic polymer⁷⁰⁻⁷⁴ also revealed significant differences in morphology and mechanical properties depending on the chemical characteristics of the polyamide phase. Blends based on nylon 6 had excellent impact properties even at low temperatures and the ABS domains were very efficiently dispersed. Blends based on nylon 6,6 were brittle and there was poor dispersion of the ABS domains.¹¹

EXPERIMENTAL

Table I provides the pertinent information about the materials used in this study. Among the four

Table I Materials Used in This Study

Designation Used Here	Commercial Designation	Composition	Molecular Weight	Relative Melt Viscosity ^a	Source
Nylon 6	Capron 8207F	End groups: NH ₂ = 47.9 μ eq/g COOH = 43.0 μ eq/g	\bar{M}_n = 22,000	1.0	Allied Signal Inc.
Nylon 6,6	Zytel 101	End groups: NH ₂ = 46.4 μ eq/g COOH = n.a.	\bar{M}_n = 17,000	1.1 ^b	E.I. Du Pont Co.
Nylon 12	AESNO TL	End groups: NH ₂ = 44.7 μ eq/g COOH = 50.5 μ eq/g	\bar{M}_n = 16,000	2.0	Atochem Inc.
Nylon 12,12	Zytel 40-401	End groups: NH ₂ = 46.0 μ eq/g COOH = n.a.	n.a.	1.5	E.I. du Pont Co.
Nylon 6/nylon 6,6 (16/84) copolymer	Vydyne 86X	End groups: NH ₂ = 49.0 μ eq/g COOH = n.a.	n.a.	1.0 ^b	Monsanto Chemical Co.
SEBS	Kraton G 1652	29% styrene	Styrene block = 7,000 EB block = 37,500	1.4	Shell Chemical Co.
SEBS-g-MA	Kraton G 1901X	29% styrene 1.84 wt % MA ^c	n.a.	1.0	Shell Chemical Co.
EPR-g-MA	None	Ethylene/propylene rubber grafted with maleic anhydride 1.5 wt % MA	500,000	1.4	Shell Chemical Co.
ABS	BL-65	SAN grafted emulsion rubber 50% rubber 24.0% AN in SAN	\bar{M}_n = 44,000 ^d \bar{M}_w = 167,000	4.0	Sumitomo Naugatuck Co.
IA-250-C	None	Imidized acrylic polymer 55.7 wt % Imide 2.18 wt % free acid 1.08 wt % anhydride	\bar{M}_w ~ 95,000	1.6	Rohm and Haas Co.

^a Brabender torque at 240°C and 60 rpm after 10 min divided by that of nylon 6.

^b Same as (a) except at 280°C.

^c Determined by elemental analysis after solvent/nonsolvent purification.

^d For the soluble SAN from GPC using polystyrene standards.

^e n.a.: not available.

different polyamides used here, only the nylon 6 has fully monofunctional character, whereas the other polyamides have some degree of difunctionality. Two of the rubbers used in this work (SEBS and SEBS-*g*-MA) are triblock copolymers that have styrene end-blocks and a hydrogenated butadiene midblock resembling an ethylene/butylene copolymer to which 1.84% maleic anhydride is grafted. The EPR-*g*-MA is an ethylene/propylene radial polymer containing 1.5% grafted maleic anhydride units. The ABS material^{10,11,75,76} is an emulsion-made product containing 50% rubber by weight with a wide distribution of particle sizes but typically in the 0.2 μm range. The SAN matrix contains 24.0% AN by weight and about 40% of the SAN is chemically grafted to the rubber. The imidized acrylic polymer, IA-250-C, used as a compatibilizer for nylon/ABS blends, is miscible with the SAN matrix of the ABS. It contains reactive acid functionality (free acid: 2.18%; anhydride: 1.08%) and 55.7% by weight glutarimide units. For rheological purposes, a Brabender Plasticorder with a 50 cm³ mixing head was used to characterize the torque at 60 rpm and at 240°C, except as noted.

Four different extruders were used for processing these blends. The single-screw extruder, a 25.4 mm Killion, also utilized in our previous work,^{5-7,9-11} was operated at a screw speed of 30 rpm. The corotating, fully intermeshing twin-screw extruders included (a) a 28 mm Werner-Pfleiderer, (b) a 25 mm Berstorff, (c) a 15 mm Baker-Perkins, and (d) a 30 mm Werner-Pfleiderer. These were operated at a screw speed of 200 rpm, except where stated otherwise. Among these, the most extensively used for this work was the 28 mm Werner-Pfleiderer twin-screw extruder, which was fitted with a "hard working" screw and had two sets of kneading blocks and reverses with a vacuum applied over the melt prior to entering the die. All extruded pellets were injection-molded into standard Izod (ASTM D256 method A) bars with

0.318 cm thickness using an Arburg Allrounder screw injection-molding machine.

Transmission electron microscopy (TEM) was used to determine blend morphology from ultrathin sections cryogenically microtomed from Izod bars perpendicular to the flow direction. The rubbers containing a styrenic phase were stained with 2% ruthenium tetroxide (RuO₄) solution.⁷⁷⁻⁸⁰ Phosphotungstic acid (PTA) was also used to selectively stain the polyamide phase.⁸¹⁻⁸⁵ The butadiene rubber phase in the ABS was stained by exposing the ultrathin microtomed samples to vapors from a 2% aqueous solution of OsO₄ for at least 8 h. A JEOL transmission electron microscope (JEM-1200EX), operated at an accelerating voltage of 120 kV, was used to view and photograph these nanometer thin sections. A semiautomatic digital image analysis technique was employed to determine the effective diameters of the dispersed phase from the TEM photomicrographs using NIH Image® software. For complex shapes of the rubber phase, the diameter assigned to each particle (including any occluded polyamide) was the average of its longest dimension and its dimension perpendicular to its major axis.⁶ No corrections were attempted to convert these apparent particle diameters into true sizes since the methods stated in the literature⁸⁶⁻⁸⁸ are not applicable for complex shapes.

RESULTS

Three different polyamide-based systems were used to compare reactive blends prepared in single screw vs. corotating twin-screw extruders. Table II shows the mechanical properties of some of the component polymers used to make these blends. The focus is primarily on the room-temperature impact strength, the ductile–brittle transition temperatures, and the morphology of these blends since these are very sensitive probes.

Table II Mechanical Properties of Key Polymers

Polymer	Izod Impact (J m ⁻¹)	Modulus (GPa)	Yield Stress (MPa)	Elongation at Break (%)
Nylon 6	40	2.8	69.6	233
Nylon 6,6	45	2.7	80.1	210
Nylon 6/Nylon 6,6 (16/84) copolymer	56	2.0	62.1	115
Nylon 12	72	1.2	41.4	250
Nylon 12,12	220	1.6	44.8	400
ABS	300	0.8	17.0	98
IA-250-C	20	3.5	89.1	5

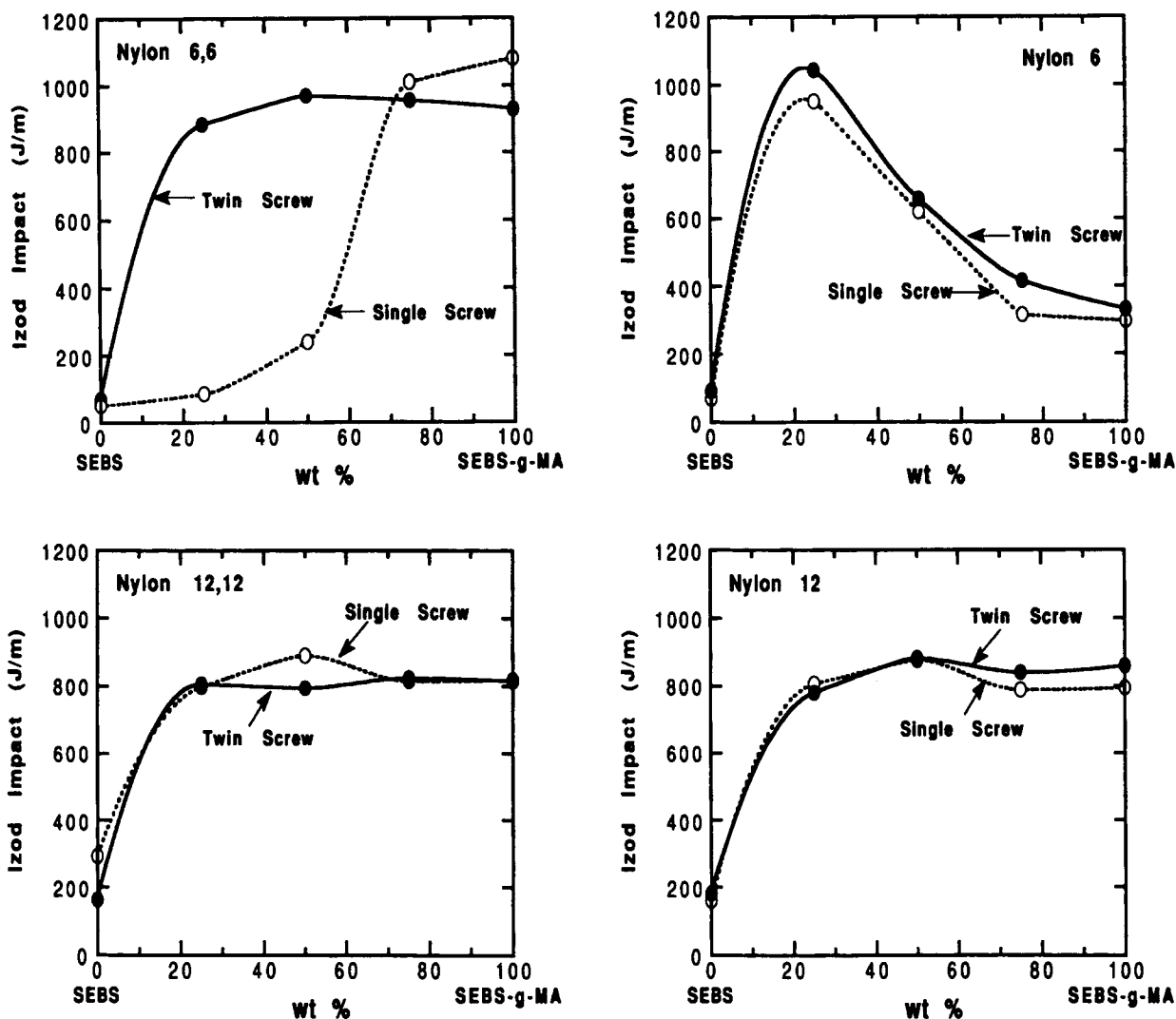


Figure 1 Impact properties of various polyamide/SEBS/SEBS-*g*-MA blends (total rubber content = 20%) prepared in 28 mm Werner-Pfleiderer twin-screw extruder (solid line) and 25.4 mm single-screw (dashed line) extruder.

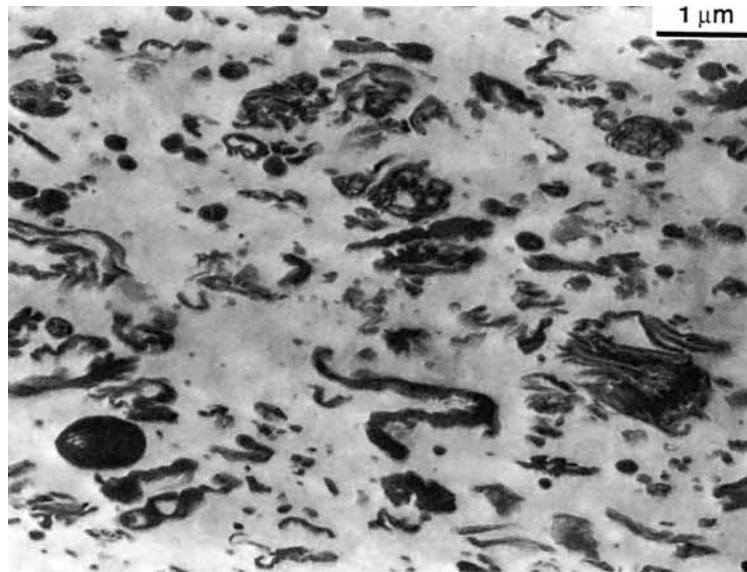
Nylon/SEBS/SEBS-*g*-MA Systems

Figure 1 compares the room-temperature impact strength of four different polyamide blends, shown as a function of the SEBS/SEBS-*g*-MA ratio, prepared in the single-screw extruder with those prepared in the 28 mm Werner-Pfleiderer twin-screw extruder. Except for nylon 6,6, the two extruders lead to very similar impact strengths. For nylon 6,6, the blends prepared in the twin-screw extruder are tough down to much lower SEBS-*g*-MA levels compared to those made in the single-screw extruder. Similar results were obtained for nylon 6,6 using the 15 mm Baker-Perkins twin-screw extruder.

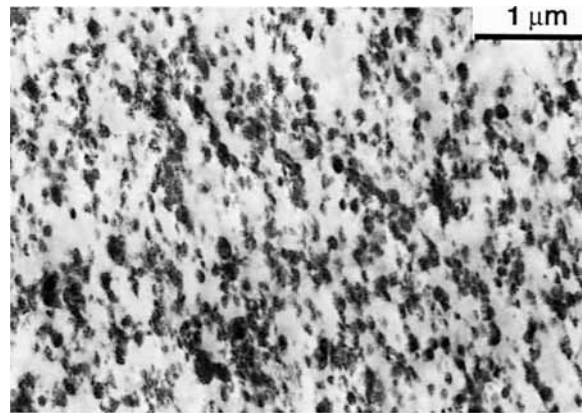
Figure 2 shows the TEM photomicrographs for

the nylon 6,6 blend containing 20% SEBS-*g*-MA prepared in three different extruders. For the single-screw extruder, extremely complex particles of the order of 1 μm are observed [Fig. 2(a)]. Although this blend is supertough at room temperature, it has poor low-temperature properties with a fraction of the samples showing brittle failure slightly below ambient temperatures.⁸⁹ Figure 2(b) and (c) show TEM photomicrographs for the same composition prepared using different twin-screw extruders. For these blends, the rubber phase is much more efficiently dispersed, with the majority of the particles in the 0.15–0.20 μm range. These blends have much better impact properties at low temperatures with ductile–brittle transition temperatures around

(a) Nylon 6,6/SEBS-g-MA (80/20)



(b) Nylon 6,6/SEBS-g-MA (80/20)



(c) Nylon 6,6/SEBS-g-MA (80/20)

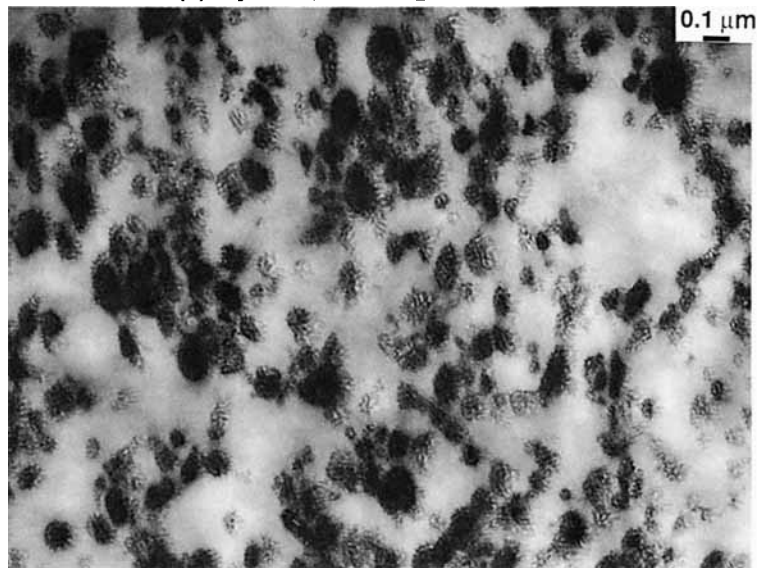
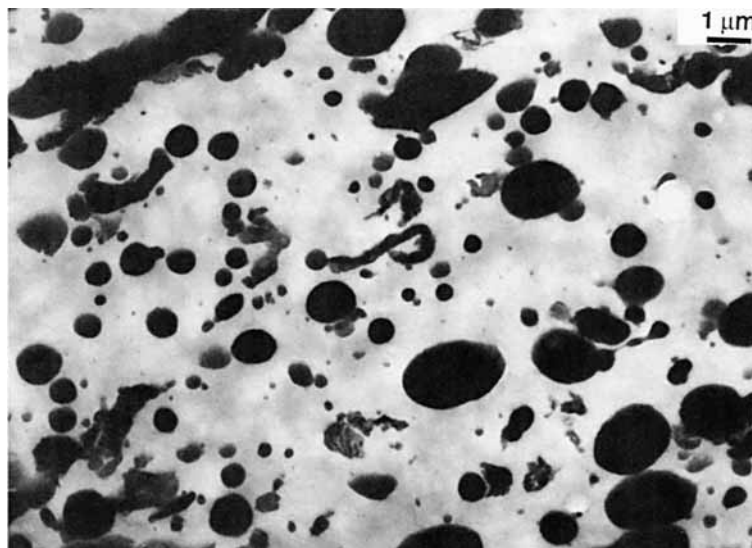


Figure 2 TEM photomicrographs of nylon 6,6/SEBS-*g*-MA (80/20) blends prepared in (a) 25.4 mm single-screw extruder ($\bar{d}_w = 0.98 \mu\text{m}$) (b) 15 mm Baker-Perkins twin-screw extruder ($\bar{d}_w = 0.20 \mu\text{m}$), and (c) 28 mm Werner-Pfleiderer twin-screw extruder—note higher magnification ($\bar{d}_w = 0.17 \mu\text{m}$). Ruthenium tetroxide (RuO_4) was employed to stain the rubber phase in these blends.

(a) Nylon 6,6/SEBS/SEBS-g-MA (80/15/5)



(b) Nylon 6,6/SEBS/SEBS-g-MA (80/15/5)

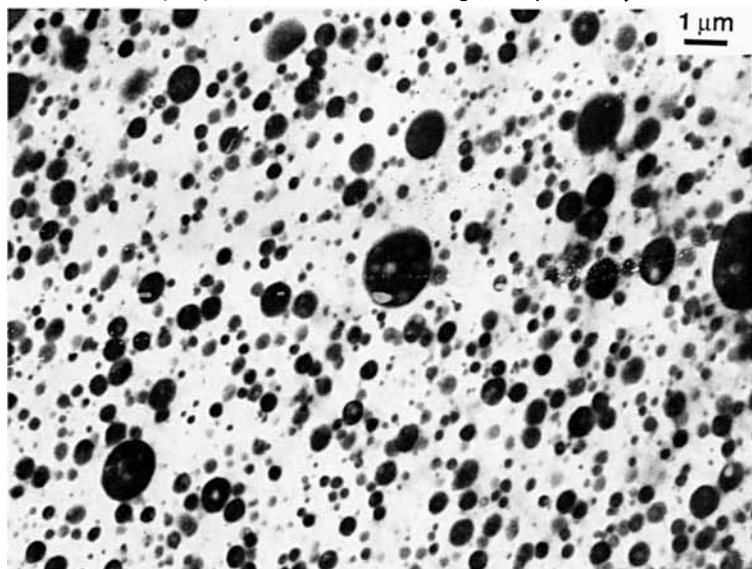


Figure 3 TEM photomicrographs of nylon 6,6/SEBS/SEBS-*g*-MA (80/15/5) blends prepared in (a) 25.4 mm single-screw extruder ($\bar{d}_w = 1.1 \mu\text{m}$) and (b) 28 mm Werner-Pfleiderer twin-screw extruder ($\bar{d}_w = 0.39 \mu\text{m}$). RuO_4 was employed to stain the rubber phase in these blends.

-10°C . Figure 3(a) and (b) compare TEM photomicrographs for nylon 6,6/SEBS/SEBS-*g*-MA (80/15/5) blends prepared in the single-screw and the 28 mm Werner-Pfleiderer twin-screw extruder, respectively. The blend prepared in the single-screw extruder is brittle at room temperature (see Fig. 1) with several particles larger than $1.0 \mu\text{m}$, as shown in Figure 3(a). Figure 3(b) shows the morphology for the same composition prepared in the 28 mm Werner-Pfleiderer twin-screw extruder. The average

particle size in this case is in the optimum range for toughening ($\bar{d}_w = 0.39 \mu\text{m}$) with the majority of the particles being spherical in shape. This blend is supertough at room temperature in contrast to the blend prepared using the single-screw extruder (see Fig. 1).

Figure 4 shows a TEM photomicrograph for a nylon 6/SEBS-*g*-MA (80/20) blend prepared in the 28 mm Werner-Pfleiderer corotating twin-screw extruder. The average particle size is $0.05 \mu\text{m}$, which

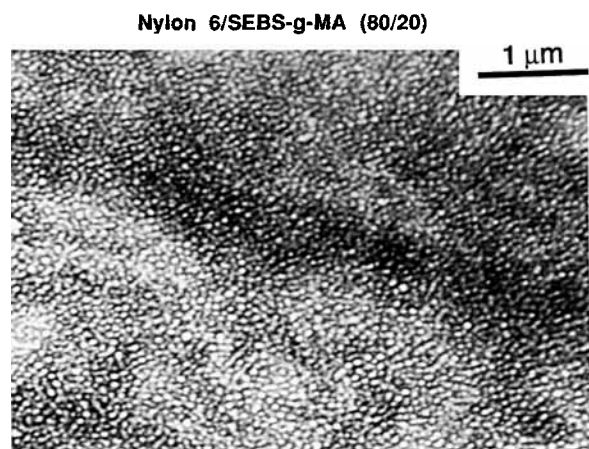
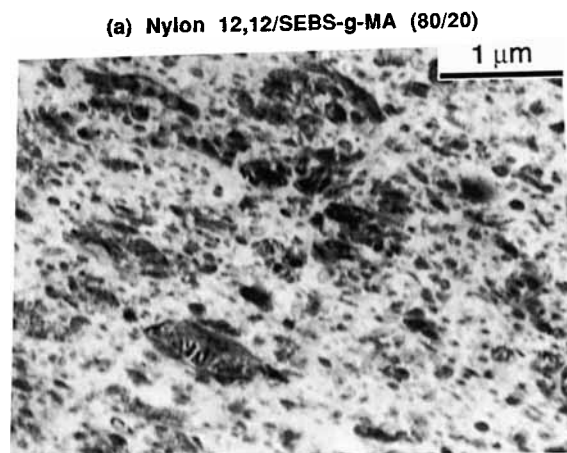


Figure 4 TEM photomicrograph of nylon 6/SEBS-*g*-MA blend prepared in a 28 mm Werner-Pfleiderer twin-screw extruder ($\bar{d}_w = 0.05 \mu\text{m}$). The polyamide phase was stained with phosphotungstic acid (PTA).

is similar to what was found in our earlier work⁷ when this composition was prepared in the single-screw extruder. As shown in Figure 1(b), both extruder types lead to blends that are rather brittle at room temperature since the rubber particle size is apparently below the lower critical limit for effective toughening.¹⁻⁸

Figure 5 compares the morphology of nylon 12,12/SEBS-*g*-MA (80/20) blends prepared using two types of extruders. For the blend prepared in the single-screw extruder, some fairly complex rubber particles ($\bar{d}_w = 0.21 \mu\text{m}$) are evident, which is attributed to the difunctional character of nylon 12,12. Using the 28 mm Werner-Pfleiderer twin-screw extruder, a much finer dispersion of the rubber phase is obtained with an average particle size of $\bar{d}_w = 0.12 \mu\text{m}$. Both blends are supertough at room temperature and have identical ductile-brittle transition temperatures (-40°C).

The above results show that for monofunctional polyamide matrices, regular spherical particles are



(b) Nylon 12,12/SEBS-*g*-MA (80/20)

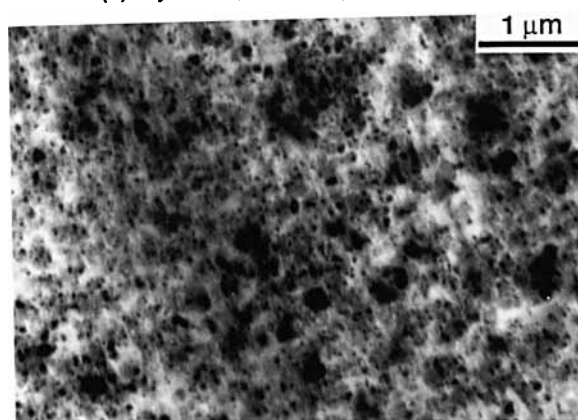


Figure 5 TEM photomicrographs of nylon 12,12/SEBS-*g*-MA (80/20) blends prepared in (a) 25.4 mm single-screw extruder ($\bar{d}_w = 0.21 \mu\text{m}$) and (b) 28 mm Werner-Pfleiderer twin-screw extruder ($\bar{d}_w = 0.12 \mu\text{m}$). RuO_4 was employed to stain the rubber phase in these blends.

generated regardless of the type of extruder employed in the processing. For the difunctional polyamides, on the other hand, significantly different rubber particle sizes and shapes are observed depending on the type of extruder used. The larger,

Table III Nylon 6/EPR-*g*-MA Blends

Impact Properties	Nylon 6-EPR- <i>g</i> -MA (80/20) (Single Step)		Nylon 6/EPR- <i>g</i> -MA (80/20) (Masterbatch)	
	Single Screw	Twin Screw	Single Screw	Twin Screw
Izod strength (J m^{-1})	665	250 ^a	848	750 ^a
Ductile-brittle transition temperature ($^\circ$)	-25	n.t. ^b	-35	$\sim -30^a$

^a From Ref. 12.

^b n.t.: not tested.

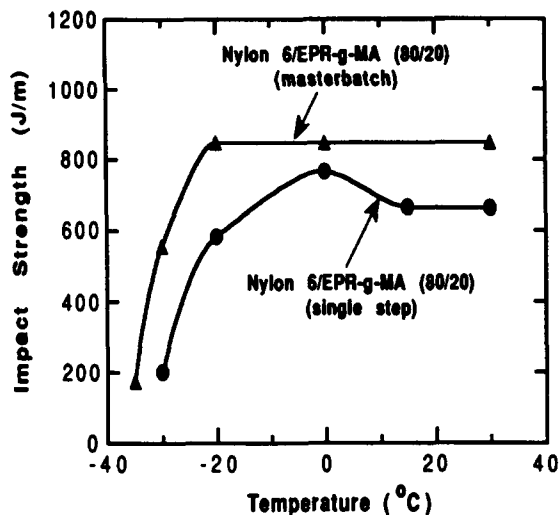


Figure 6 Impact strength as a function of temperature for nylon 6/EPR-*g*-MA (80/20) blends prepared in a single-screw extruder.

complex particles for the nylon *x,y* blends prepared in the single-screw extruder are obviously a consequence of the relatively lower mixing intensity in this device, which is not capable of breaking up the cross-linked rubber phase formed in these systems. In the case of nylon 6,6, this translates to a lower ductile-brittle transition temperature, whereas the low-temperature impact properties of nylon 12,12 blends are insensitive to such morphological differences. This is probably a consequence of the much higher inherent ductility of nylon 12,12 stemming from its high methylene content in the repeat unit (CH_2/NHCO ratio).

Nylon/EPR-*g*-MA blends

Modic and Pottick¹² recently described the properties of blends of nylon 6 and nylon 6,6 with a maleated ethylene/propylene rubber (designated here as EPR-*g*-MA) prepared in a 25 mm Berstorff twin-screw extruder operated at 300 rpm. Blends of this rubber with nylon 6,6 showed better impact performance than that of the corresponding blends with the SEBS-*g*-MA material. However, after a single pass through the twin-screw extruder, blends of this rubber with nylon 6 had rubber particles below the critical size for effective toughening, similar to previous observations with SEBS-*g*-MA.⁵⁻⁷ Tough blends of EPR-*g*-MA with nylon 6 could, however, be generated through a masterbatch technique that involved preparing a nylon/rubber concentrate that was then diluted with more nylon 6 in a second extrusion step to give a final composition that had

20% rubber. This mixing protocol led to enlarged rubber particles, via polyamide occlusions, in the optimum size range for toughening.¹²

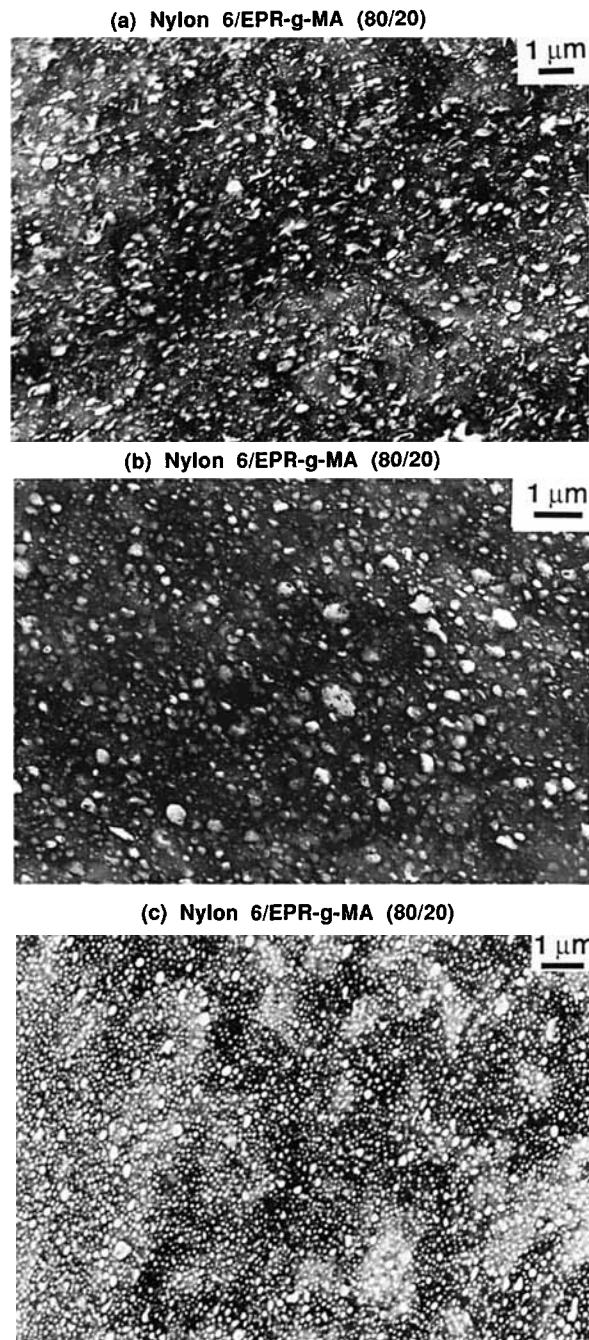
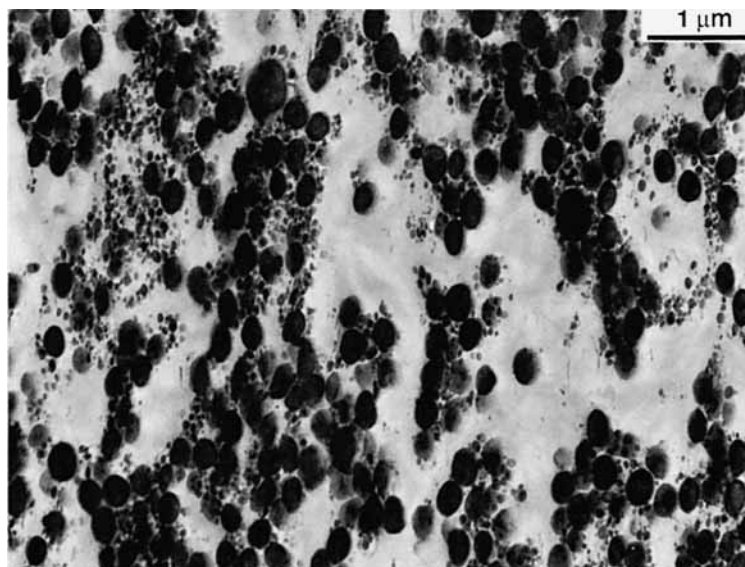


Figure 7 TEM photomicrographs of nylon 6/EPR-*g*-MA (80/20) blends prepared by (a) single pass in a 25.4 mm single-screw extruder ($\bar{d}_w = 0.30 \mu\text{m}$), (b) masterbatch technique in a 25.4 mm single-screw extruder ($\bar{d}_w = 0.22 \mu\text{m}$), and (c) single pass in a 25 mm Berstorff twin-screw extruder ($\bar{d}_w = 0.08 \mu\text{m}$). The polyamide phase was stained with PTA in these blends.

(a) Nylon 6,6/ABS/IA-250-C (45/45/10)



(b) Nylon 6,6/ABS/IA-250-C (45/45/10)

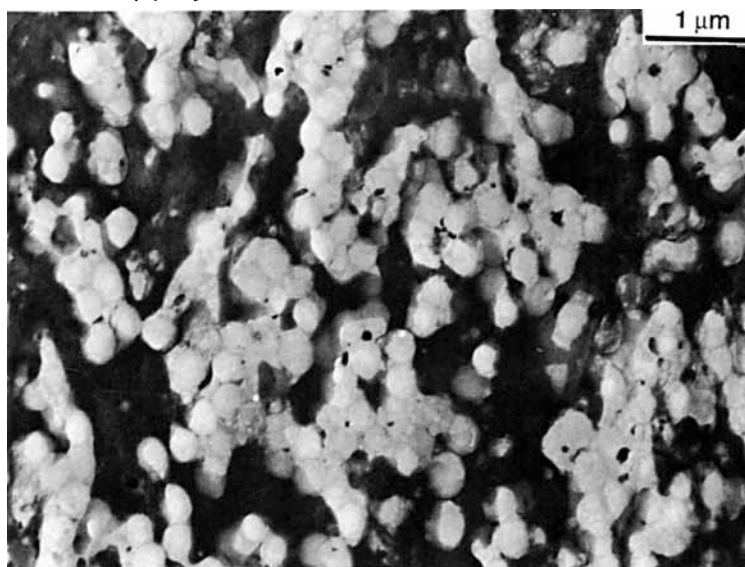


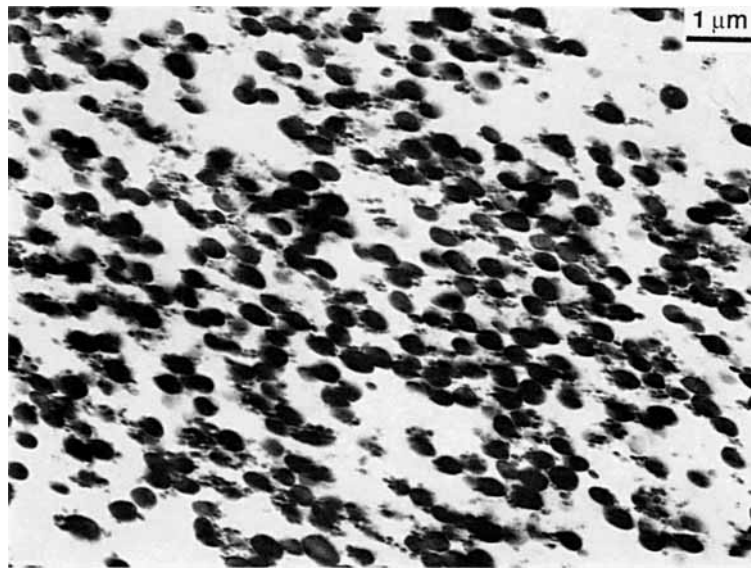
Figure 8 TEM photomicrographs for nylon 6,6/ABS/IA-250-C (45/45/10) blends prepared in (a) 25.4 mm single-screw extruder (stained with OsO_4), (b) 25.4 mm single-screw extruder (stained with PTA), (c) 15 mm Baker-Perkins twin screw (stained with OsO_4), and (d) 15 mm Baker-Perkins twin screw (stained with PTA).

Table III compares the mechanical properties of nylon 6/EPR-*g*-MA blends prepared in the Killion single-screw extruder with those reported by Modic and Pottick.¹² The masterbatch technique involved preparing a 40/60 nylon 6/EPR-*g*-MA blend, which was then diluted with nylon 6 in the second step to the desired 80/20 ratio. The mechanical properties of this blend prepared by the masterbatch technique and the single-step operation are not so dramatically

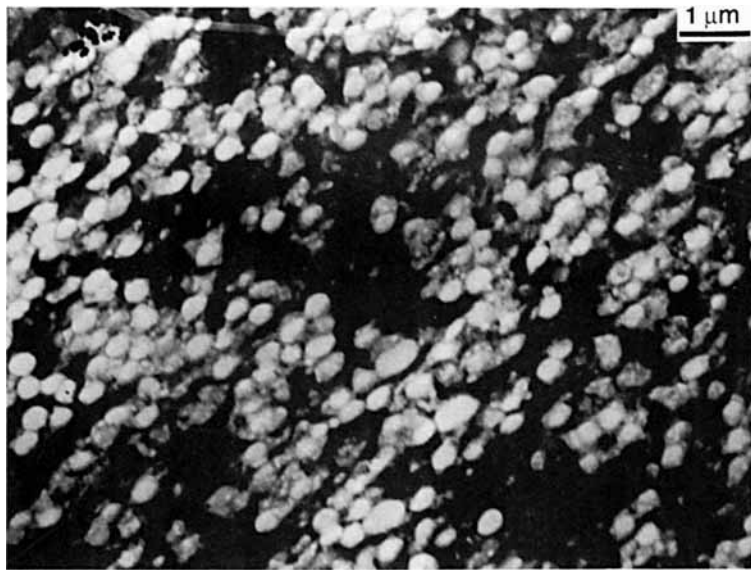
different when the compounding is done in a single-screw extruder (see Table III). Both mixing protocols lead to toughened blends with excellent low temperature properties, as shown in Figure 6.

Figure 7(a)–(c) show TEM photomicrographs for some of the blends shown in Table III utilizing phosphotungstic acid (PTA) to stain the polyamide phase. For the blend prepared in the single-screw extruder, most rubber particles are finely dispersed

(c) Nylon 6,6/ABS/IA-250-C (45/45/10)



(d) Nylon 6,6/ABS/IA-250-C (45/45/10)

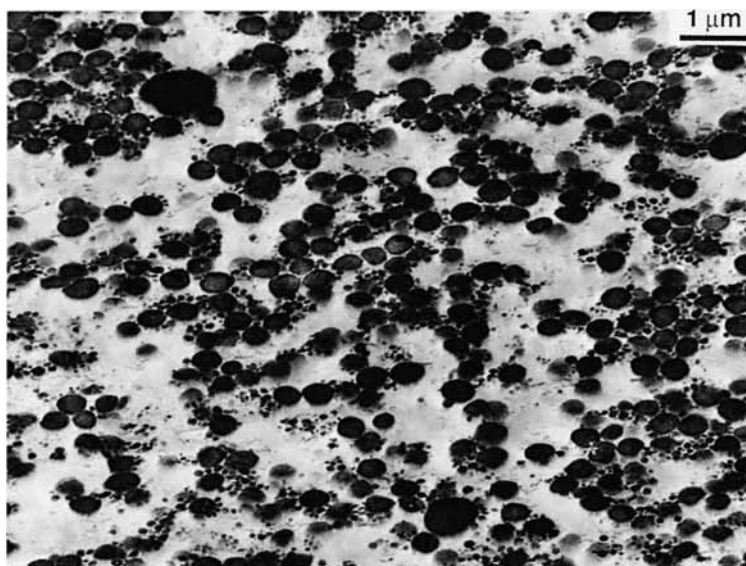
**Figure 8** (Continued from the previous page)

($\bar{d}_w \sim 0.30 \mu\text{m}$), but a significant fraction of the particles have fairly complex shapes [Fig. 7(a)]. The blends prepared in the single-screw extruder by the masterbatch technique show well-dispersed rubber particles with a significant number having polyamide occlusions inside them [Fig. 7(b)]. This is similar to the observations of Modic and Pottick¹² for similar nylon 6/EPR-*g*-MA blends prepared by the same masterbatch technique in their twin-screw extruder. Figure 7(c) shows a TEM photomicrograph for a blend prepared in the twin-screw extruder

used by Modic and Pottick using a one-step operation. The rubber particles are much more finely dispersed ($\bar{d}_w = 0.08 \mu\text{m}$) and more regular in shape than for the corresponding blend formed in the single-screw extruder [Fig. 7(a)].

It is clear from the above discussion that the morphology of nylon 6/EPR-*g*-MA blends is quite sensitive to the mixing protocol and processing conditions. The single-screw extruder gives better impact strength for a single pass operation since the lower intensity of mixing provided by this device

(a) Vydyne 86X/ABS/IA-250-C (45/45/10)



(b) Vydyne 86X/ABS/IA-250-C (45/45/10)

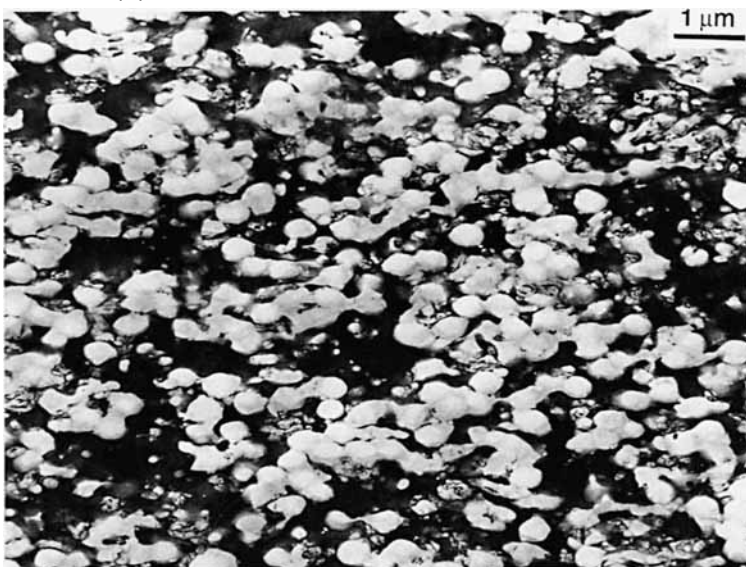
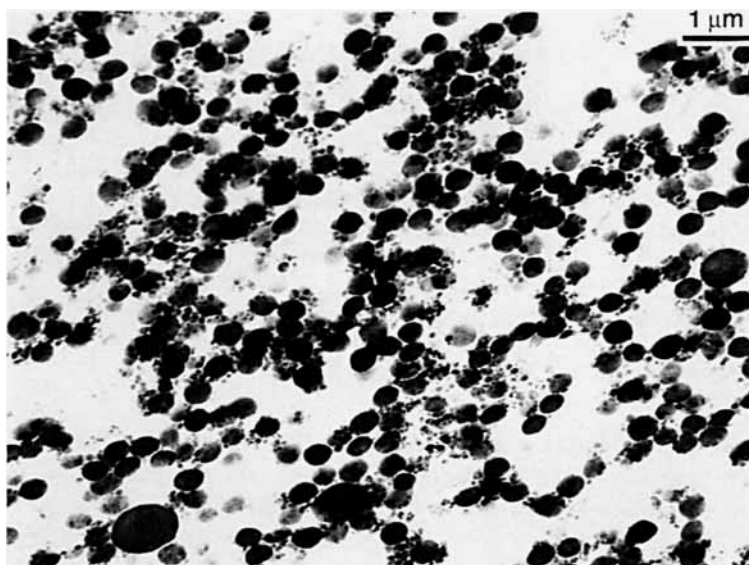


Figure 9 TEM photomicrographs for Vydyne 86X/ABS/IA-250-C (45/45/10) blends prepared in (a) 25.4 mm single-screw extruder (stained with OsO_4), (b) 25.4 mm single-screw extruder (stained with PTA), (c) 15 mm Baker-Perkins twin screw (stained with OsO_4), and (d) 15 mm Baker-Perkins twin screw (stained with PTA).

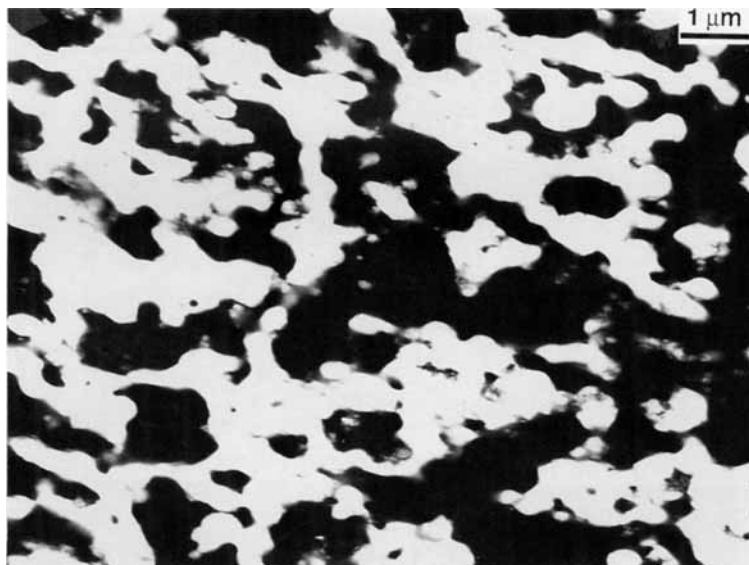
does not break down the rubber particles to dimensions below the critical limit for toughening nylon 6. This is in contrast to nylon 6/SEBS-*g*-MA blends where the rubber particles generated in both single- and twin-screw extruders are significantly below the critical limit for toughening. A significant factor in these differences is that the EPR-*g*-MA has a much higher molecular weight and a somewhat higher melt viscosity than those of the SEBS-*g*-MA (see Table I). The EPR-*g*-MA contains about the same amount

of maleic anhydride as does the SEBS-*g*-MA, so there are significantly more maleic anhydride sites per chain at which nylon linkages can form. These and possibly other factors impede the rate of drop breakup and form complex particles in the single-screw extruder where the intensity of mixing is relatively low, but, apparently, the more intense mixing in the twin-screw extruder is sufficient to break these complex shapes into small, regular particles in a one-step operation.

(c) Vydne 86X/ABS/IA-250-C (45/45/10)



(d) Vydne 86X/ABS/IA-250-C (45/45/10)

**Figure 9** (Continued from the previous page)

Compatibilized Nylon/ABS Blends

Table IV compares the mechanical properties of nylon/ABS blends, reactively compatibilized with the imidized acrylic polymer⁷⁰⁻⁷⁴ described in Table I, prepared in two different twin-screw extruders (the 15 mm Baker-Perkins and the 30 mm Werner-Pfleiderer) and the 25.4 mm Killion single-screw extruder. The polyamide phase in these blends is either the nylon 6,6 or nylon 6/nylon 6,6 copolymer (Vydne 86X) described in Table IV. The impact properties of these blends are essentially independent of the type of extruder in which they are made. Both extruder types lead to brittle blends in the case

of nylon 6,6, whereas the blends based on the nylon 6/nylon 6,6 copolymer are tough at room temperature but become brittle slightly below this ($\sim 12^\circ\text{C}$).

TEM photomicrographs for the blends based on nylon 6,6 and the nylon 6,6/nylon 6 copolymer shown in Figures 8 and 9 do not reveal significant differences in the degree of dispersion of the ABS phase between the blends prepared in the two types of extruders. Both staining techniques show very large ABS domains for these blends; however, the phosphotungstic acid (PTA) staining gives a precise identification of the nylon/ABS boundaries. By comparison, the dispersion of the ABS domains is

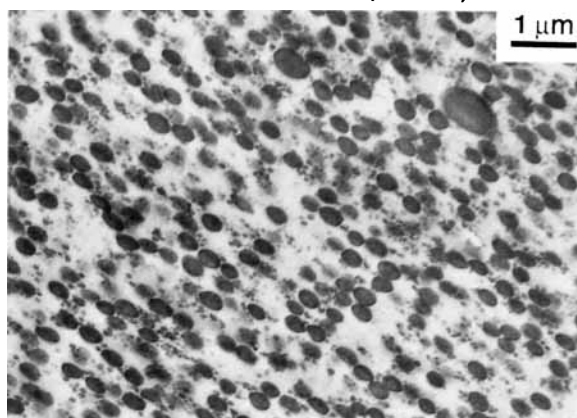
Table IV. Nylon *x,y*/ABS Blends

Blend	Extruder Type	Impact Strength (J m ⁻¹)	Ductile–Brittle Transition Temperature (°C)
Nylon 6,6/ABS/IA-250-C (45/45/10)	25.4 mm Killion single screw	150	65
Nylon 6,6/ABS/IA-250-C (45/45/10)	15 mm Baker-Perkins twin screw	160	55
Nylon 6,6/ABS/IA-250-C (45/45/10)	30 mm Werner-Pfleiderer twin screw	160	55
Vydyne 86X/ABS/IA-250-C (45/45/10)	25.4 mm Killion single screw	745	12
Vydyne 86X/ABS/IA-250-C (45/45/10)	15 mm Baker-Perkins twin screw	750	12

much more efficient for 6/ABS blends processed in a single-screw extruder (see Fig. 10). The latter blend is supertough down to relatively low temperatures (-10°C).¹⁰

The mechanical properties and morphology of reactively compatibilized blends of ABS with difunctional polyamides cannot be improved by use of the more intense mixing provided by a twin-screw

(a) Nylon 6/ABS/IA-250-C (45/45/10)



(b) Nylon 6/ABS/IA-250-C (45/45/10)



Figure 10 TEM photomicrograph for nylon 6/ABS/IA-250-C (45/45/10) blend prepared in 25.4 mm single-screw extruder stained with (a) OsO_4 and (b) PTA.

extruder, which is contrary to what was shown for blends of similar polyamides with SEBS-*g*-MA and EPR-*g*-MA earlier in this article. This difference may be related to the higher viscosity of the ABS material. However, using the same compatibilizer, excellent dispersion of ABS in monofunctional nylon 6 can be achieved in a single-screw extruder.

CONCLUSIONS

The examples described here demonstrate that for optimizing the toughness properties of reactive polyamide blends the choice of mixing intensity or extruder type must be decided on a case-by-case basis. The more intense mixing provided by typical corotating twin-screw extruders is not always necessary or desirable. This stems from the fact that there generally is an optimum morphology for toughening and the degree of dispersion can be either too fine or too coarse for optimal performance. In addition, the intensity of mixing needed to achieve a given degree of dispersion in reactive systems depends on several factors including issues of chemical topology in addition to the usual ones of rheology, interfacial tension, etc. For example, while a corotating twin-screw extruder is more effective in dispersing the rubber phase in the difunctional polyamide-based blends (nylon 6,6/SEBS-*g*-MA), it fails to achieve this in the case of compatibilized nylon 6,6/ABS blends. In general, monofunctional polyamide blends are less sensitive to the extruder type used to process them, as demonstrated here for a number of different systems.

These results, no doubt, have a broader significance in selecting extruders for reactively compatibilizing polymer blends, since cost of the processing equipment is often a major consideration in addition to performance of the product. From the observations reported here, it is evident that less expensive single-screw extruders can match the performance of corotating twin-screw extruders for some systems but not for others.

The research was supported by the U.S. Army Research Office. The authors are indebted to Dr. E. A. Flexman of DuPont, Mr. M. J. Modic of Shell Development Co., and Drs. N. G. Harvey and C. Hesler at Rohm and Haas Co. for their assistance with blend preparation and materials. The assistance of Mr. D. Kallick at the University of Texas Photography Department is greatly appreciated.

REFERENCES

1. D. Gilmore and M. J. Modic, *SPE ANTEC Tech. Pap.*, **35**, 1371 (1989).
2. M. J. Modic, D. W. Gilmore, and J. P. Kirkpatrick, in *Proceedings of the First International Congress on Compatibilization and Reactive Polymer Alloying (Compalloy '89)*, New Orleans, LA, 1989, p. 197.
3. M. J. Modic and L. A. Pottick, *Polym. Eng. Sci.*, **33**, 819 (1993).
4. R. Gelles, M. J. Modic, and J. Kirkpatrick, *SPE ANTEC Tech. Pap.*, **34**, 513 (1988).
5. A. J. Oshinski, H. Keskkula, and D. R. Paul, *Polymer*, **33**, 268, 284 (1992).
6. Y. Takeda, H. Keskkula, and D. R. Paul, *Polymer*, **33**, 3173 (1992).
7. B. Majumdar, H. Keskkula, and D. R. Paul, *Polymer*, **35**, 1386, 1399 (1994).
8. A. J. Oostenbrink, L. J. Molenaar, and R. J. Gaymans, Poster given at 6th Annual Meeting of Polymer Processing Society, Nice, France, April, 18–20, 1990.
9. B. Majumdar, H. Keskkula, and D. R. Paul, *Polymer*, in press.
10. B. Majumdar, H. Keskkula, and D. R. Paul, *Polymer*, in press.
11. B. Majumdar, H. Keskkula, and D. R. Paul, *Polymer*, in press.
12. M. J. Modic and L. A. Pottick, *Plast. Eng.*, **7**, 37 (1991).
13. Z. Tadmor and C. G. Gogos, *Principles of Polymer Processing*, Wiley, New York, 1979.
14. C. Rauwendaal, *Polymer Extrusion*, Hanser, New York, 1986.
15. F. G. Martelli, *Twin Screw Extruders: A Basic Understanding*, Van Nostrand Reinhold, New York, 1983.
16. K. Min, J. L. White, and J. F. Fellers, *Polym. Eng. Sci.*, **24**, 1327 (1984).
17. J. L. White, W. Szydlowski, K. Min, and M. H. Kim, *Adv. Polym. Technol.*, **7**, 295 (1987).
18. J. L. White, J. K. Kim, W. Szydlowski, and K. Min, *Polym. Compos.*, **9**, 368 (1988).
19. D. K. Setua, S. Lim, and J. L. White, *SPE ANTEC Tech. Pap.*, **38**, 2686 (1992).
20. T. Sakai, N. Hashimoto, and N. Kobayashi, *SPE ANTEC Tech. Pap.*, **33**, 146 (1987).
21. L. A. Utracki, *Polymer Alloys and Blends—Thermodynamics and Rheology*, Hanser, Munich, 1989.
22. L. A. Utracki and Z. H. Shih, *Polym. Eng. Sci.*, **32**, 1824, 1834 (1992).
23. V. Bordereau, Z. H. Shi, L. A. Utracki, P. Sammut, and M. Carrega, *Polym. Eng. Sci.*, **32**, 1846 (1992).
24. J. T. Lindt, *Polym. Eng. Sci.*, **21**, 1162 (1981).
25. H. Fukas, T. Kunio, S. Shinya, and A. Nomura, *Polym. Eng. Sci.*, **22**, 587 (1982).
26. P. H. M. Elmans, PhD thesis, Eindhoven University of Technology, The Netherlands, 1989.
27. P. H. M. Elmans, Van Gisebersgen, and H. E. M. Meijer, in *Integration of Fundamental Polymer Science and Technology-2*, P. J. Lemstra and L. A. Kleintjens, Eds., Elsevier, London, 1988, p. 261.
28. H. E. M. Meijer and P. H. M. Elmans, *Polym. Eng. Sci.*, **28**, 2751 (1988).
29. P. H. M. Elmans, J. M. Jansen, and H. E. M. Meijer, *J. Rheol.*, **34**, 1311 (1990).

30. B. D. Favis, *J. Appl. Polym. Sci.*, **39**, 285 (1990).
31. J. M. Willis, V. Caldas, and B. D. Favis, *J. Mater. Sci.*, **26**, 4742 (1991).
32. B. D. Favis, *Can. J. Chem. Eng.*, **69**, 619 (1991).
33. B. D. Favis and D. Therrien, *Polymer*, **32**, 1474 (1991).
34. S. Wu, *Polym. Eng. Sci.*, **27**, 335 (1987).
35. G. Serpe, J. Jarrin, and F. Dawans, *Polym. Eng. Sci.*, **30**, 553 (1990).
36. B. D. Favis and J. P. Chalifoux, *Polym. Eng. Sci.*, **27**, 1591 (1987).
37. H. J. Van Oene, *J. Coll. Interf. Sci.*, **40**, 448 (1978).
38. C. D. Han and K. Funatsu, *J. Rheol.*, **22**, 113 (1978).
39. G. I. Taylor, *Proc. R. Soc. Lond. A*, **138**, 41 (1932).
40. G. I. Taylor, *Proc. R. Soc. Lond. A*, **146**, 501 (1934).
41. W. Bartok and S. G. Mason, *J. Colloid Sci.*, **13**, 393 (1958).
42. W. Bartok and S. G. Mason, *J. Colloid Sci.*, **14**, 13 (1959).
43. F. D. Rumscheidt and S. G. Mason, *J. Colloid Sci.*, **16**, 238 (1961).
44. S. Torza, R. C. Cox, and S. G. Mason, *J. Colloid Interf. Sci.*, **38**, 395 (1972).
45. H. P. Grace, *Chem. Eng. Commun.*, **14**, 225 (1982).
46. M. Von Smoluchowski, *Z. Phys. Chem.*, **92**, 129 (1917).
47. M. Von Smoluchowski, *Phys. Z.*, **17**, 557, 585 (1916).
48. N. Tokita, *Rubb. Chem. Tech.*, **50**, 292 (1977).
49. J. J. Elmendorp and A. K. Van der Vegt, *Polym. Eng. Sci.*, **26**, 1332 (1986).
50. I. Fortelny and J. Kovar, *Polym. Compos.*, **9**, 119 (1988).
51. U. Sundararaj, C. W. Macosko, R. J. Rolando, and H. T. Chan, *Polym. Eng. Sci.*, **32**, 1814 (1992).
52. C. E. Scott and C. W. Macosko, *Polym. Bull.*, **26**, 341 (1991).
53. T. Nishio, Y. Suzuki, K. Kojima, and M. Kakugo, in *The 7th Annual Meeting, PPS*, Hamilton, Canada, April 22-24, 1991.
54. T. Sanada, T. Ogifara, Y. Suzuki, and T. Nishio, in *PPS European Meeting*, Palermo, Italy, Sept. 15-18, 1991.
55. A. K. Ghosh, S. Ranganathan, J. T. Lindt, and S. Lorek, *SPE ANTEC Tech. Pap.*, **37**, 99 (1991).
56. A. P. Plochocki, S. S. Dagli, and R. D. Andrews, *Polym. Eng. Sci.*, **30**, 741 (1990).
57. D. B. Todd, in *Reactive Extrusion*, M. Xanthos, Ed., Hanser, Munich, 1992.
58. Ph. Teyssie, *Makromol. Chem. Macromol. Symp.*, **22**, 83 (1988).
59. S. D. Sjoerdsma, A. C. A. M. Bleijenberg, and D. Heikens, *Polymer*, **22**, 619 (1981).
60. R. Jerome, R. Fayt, and Ph. Teyssie, in *Thermoplastic Elastomers: A Comprehensive Review*, N. R. Legge, H. Schroeder, and G. Holden, Eds., Hanser Verlag, Munich, 1987, Chap. 12, Sec. 7.
61. D. R. Paul, in *Thermoplastic Elastomers: A Comprehensive Review*, N. R. Legge, H. Schroeder, and G. Holden, Eds., Hanser Verlag, Munich, 1987, Chap. 12, Sec. 6.
62. M. Xanthos, *Polym. Eng. Sci.*, **28**, 1392 (1988).
63. N. C. Liu and W. E. Baker, *Adv. Polym. Technol.*, **11**, 249 (1992).
64. S. Wu, *Polymer*, **26**, 1855 (1985).
65. S. Y. Hobbs, R. C. Bopp, and V. H. Watkins, *Polym. Eng. Sci.*, **23**, 380 (1983).
66. M. W. Fowler and W. E. Baker, *Polym. Eng. Sci.*, **28**, 1427 (1988).
67. R. J. M. Borggreve and R. J. Gaymans, *Polymer*, **30**, 63 (1989).
68. R. J. M. Borggreve, R. J. Gaymans, and J. Schuijjer, *Polymer*, **30**, 71 (1989).
69. R. J. M. Borggreve, R. J. Gaymans, and A. R. Luttmmer, *Makromol. Chem. Macromol. Symp.*, **16**, 195 (1988).
70. M. Hallden-Abberton, U.S. Pat. 4,246,374 (1989) (to Rohm and Haas).
71. M. Hallden-Abberton, *Polym. Mater. Sci. Eng.*, **65**, 361 (1991).
72. M. Hallden-Abberton, L. Cohen, and R. Wood, U.S. Pat. 4,874,824 (1989) (to Rohm and Haas).
73. M. Hallden-Abberton, N. Bortnick, L. Cohen, W. Freed, and H. Fromuth, U.S. Pat. 4,727,117 (1988) (to Rohm and Haas).
74. M. E. Fowler, D. R. Paul, L. A. Cohen, and W. T. Freed, *J. Appl. Polym. Sci.*, **37**, 513 (1989).
75. H. Kim, H. Keskkula, and D. R. Paul, *Polymer*, **31**, 869 (1990).
76. J. H. Kim, H. Keskkula, and D. R. Paul, *J. Appl. Polym. Sci.*, **40**, 183 (1990).
77. J. S. Trent, *Macromolecules*, **17**, 2930 (1984).
78. J. S. Trent, J. I. Scheinbeim, and P. R. Couchman, *Macromolecules*, **16**, 589 (1983).
79. J. S. Trent, J. I. Scheinbeim, and P. R. Couchman, *J. Polym. Sci. Polym. Lett. Ed.*, **19**, 315 (1981).
80. R. Vitali and E. Montani, *Polymer*, **21**, 1220 (1980).
81. J. Martinez-Salazar and C. G. Cannon, *J. Mater. Sci. Lett.*, **3**, 693 (1984).
82. D. E. Morel and D. T. Grubb, *Polymer*, **25**, 41 (1984).
83. E. K. Boylston and M. L. Rollins, *Microscope*, **19**, 255 (1971).
84. B. J. Spit, *Faserforsch. Textiltech.*, **18**, 161 (1967).
85. J. A. Rusnock and D. Hansen, *J. Polym. Sci. Part A*, **3**, 617 (1965).
86. E. M. Chamot and C. W. Mason, in *Handbook of Chemical Microscopy*, Wiley, London, 1983.
87. G. Bach, in *Qualitative Methods in Morphology*, Springer-Verlag, Berlin, 1967.
88. K. Mihira, T. Ohsawa, and A. Nakayamu, *Kolloid. Z.*, **222**, 135 (1968).
89. B. Majumdar, PhD Dissertation, University of Texas at Austin, 1993.

Received December 28, 1993

Accepted April 12, 1994